

Introduction

For the electron linac the principal problems of the acceleration dynamics are confined to the "front end" or what is usually denoted as the injector. The high charge-to-mass ratio of the electron guarantees that, after a meter or so under modest accelerating gradients, the electron beam becomes so rigid that problems of beam transport are decoupled from problems of acceleration. The emittance of the electron beam from the whole accelerator is therefore determined principally by the emittance from the injector. Also regenerative beam instabilities and space-charge effects are most severe at the low energies of the injector.

The injector system for the Stanford superconducting accelerator^{1,2} was designed to meet the original goal of producing an electron beam of 100 μ a with an energy resolution of 10^{-4} for final energies from the accelerator of 1 GeV or more. Now after having operated and measured the beam performance of the injector, we believe that by operating the injector in a mode slightly different from that originally anticipated, we can approach the 10^{-4} resolution goal at final energies as low as 100 MeV.

Injector System

The injector system is shown schematically in Fig. 1. In the original mode of operation, 80 keV electrons are generated from a triode gun which operates from a highly stabilized 80 kV power supply. The electron beam passes through apertures which limit the transverse properties to acceptable levels. A pair of room-temperature rf cavities (chopper cavities) sweep the beam in an elliptical scan across an aperture at the basic frequency of the accelerator (1300 MHz). The chopped beam (nominally 30 degrees) then passes through another room-temperature rf cavity (prebuncher) which produces bunching of the phase so that at the point of entry into the first accelerator structure the total spread in phase and energy is less than 10 degrees and 2 keV, respectively.

The capture section is the first superconducting accelerating structure encountered by the 80 keV beam. This 7-cell, 0.8 m long, niobium structure accelerates the electrons to an energy of a few MeV where they then pass into the preaccelerator structure. The preaccelerator, a 23-cell, 2.4 m structure, further accelerates the electrons completing the bunching process and providing a stiff, relativistic beam for injection into the accelerator.

Before being injected into the main portion of the accelerator the electron beam first passes through the beam filter³ which is a beam transport system consisting of four bending magnets, several solenoidal lenses, and several adjustable slits. This isochronous transport system permits the filtering out of any low-energy electrons such as those generated, for example, by field emission from either the capture or preaccelerator section.

Besides the usual reasons for a "clean" beam at injection, we must conserve refrigeration at 1.85°K. As a bonus, the transporting, filtering, and recirculating of the high-energy beam is facilitated.

Recirculation of the electron beam through the accelerator will be utilized to increase the maximum energy produced by the accelerator. The beam filter in this respect provides the necessary displacement and deflections of the injector beam so that the recirculated beam can be brought into proper alignment for reinjection into the accelerator.

The beam analyzing apparatus, shown in Fig. 1, consists of a superconducting accelerator structure and a magnetic spectrometer. This accelerator structure was used to measure the spread in phase of the beam by operating 90° from the peak acceleration. A peak energy gain of 600 keV provided a dispersion of 10 keV per rf degree. The spread in energy was measured with the magnetic spectrometer system. The intrinsic momentum resolution of this system, including beam-size effects, was estimated to be $\Delta p/p \approx 0.02\%$.

Design Considerations

A spread in phase $\Delta\phi$ of the electrons from the injector will contribute to the spread in energy from the accelerator by an amount given by

$$\frac{\Delta E}{E} \approx \frac{(\Delta\phi)^2}{8} \tag{1}$$

If the fluctuations of the rf accelerating fields are limited to 5 parts in 10^{-5} and the effective injection phase is held constant to approximately 0.2 degrees, a $\Delta\phi$ of one degree would be necessary to limit the total spread in energy to 10^{-4} .

Our actual design is to have $\Delta E/E = 10^{-4}$ full-width-at-half-maximum (FWHM) and to have 80% or more within $\Delta E/E = 2 \times 10^{-4}$. To meet this condition we require that 90% of the electrons fall within $\Delta\phi = 1.5^\circ$. In addition, the initial energy spread must be held to 50 keV at injection to get a $\Delta E/E$ of 10^{-4} at 1 GeV.

The original design of the capture section and the analysis of the bunching properties were based on an accelerating field strength of 10 MV/m. Shown in Fig. 2 is the calculated⁴ transfer function of the capture section for the longitudinal phase space for electrons at 80 keV limited to spreads in phase and energy of ± 6 degrees and ± 0.8 keV respectively. With the preaccelerator section phased so that the incident electron would arrive a few degrees ahead of peak acceleration, the phase space distribution would be sheared with respect to energy (vertically in Fig. 2) giving an output falling inside the bounds of $\Delta\phi = 1.2$ degrees and $\Delta E = 28$ keV.

The parameters of the 80 keV system were chosen to meet the requirement that electrons be produced with an energy spread less than ± 0.8 keV

and a phase spread less than ± 0.6 degrees. Both rf phase chopping⁵ and prebunching were considered to be necessary to meet the longitudinal phase space requirements without having to throw too much of the beam away. Two TM₁₂₀ mode rectangular cavities are employed to produce an elliptical scan of the electron beam across an aperture. For this simple system of chopping there is a strong coupling of the transverse and longitudinal phase spaces. If the beam direction is assumed to be the positive Z axis and the beam is being deflected in the Y direction by the magnetic field component $H_{x0} \sin \omega t$, there will be a gradient in the Z component of the electric field given by

$$\frac{\partial E_z}{\partial y} = \mu_0 \omega H_{x0} \cos \omega t . \quad (2)$$

The finite dimension of the beam in the Y direction (while passing through the chopper cavity) will therefore contribute to the energy spread. In the region of linear chopping, the longitudinal phase space area is proportional to the transverse phase space of the beam entering the chopper system. For our system at 80 keV, a transverse phase-space area of 20 mm. mrad leads to a longitudinal phase-space area of 20 keV-degrees. If the beam spot diameter at the chopping aperture is approximately the same as that of the aperture, for a chopped bunch of mean width 30 degrees there will be maximum phase deviations of ± 30 degrees. The total phase-space area of 20 keV-degrees is bounded therefore by a phase deviation of ± 30 degrees and an energy deviation of ± 166 volts. Approximately 10 watts of rf power is required to produce the necessary field levels in each of the copper plated, stainless steel chopper cavities.

The 60 degree by 333 volt phase-space area is transformed into the desired 12 degree by 1600 volt configuration by the prebuncher and a suitable drift length. In this case, the buncher gradient required is 27 volts per degree (1.5 keV voltage gain at the peak) and the drift length required is 2.3 m. For our copper, re-entrant, TM₀₁₀ cavity, only 1.5 watts of rf power is necessary to produce these field strengths.

The electrons from the gun must be stable enough in energy so that the contribution to the spread in phase is not serious. The stability requirement of ± 20 volts on the 80 kV power supply was deemed adequate. In 3 meters of drift length, for example, 20 volts of modulation corresponds to a phase modulation of 0.9 degree.

With respect to the transverse phase space, the original design goals were not as well defined as were the goals for the longitudinal phase space. If the coupling from transverse to the longitudinal spaces could be shown to be small, restrictions in the transverse phase space would be those coming from the considerations of obtaining transport of the beam through the accelerator without loss of current, of adequate resolution in beam analyzing equipment, and of course, the physics experiments (e.g., high-resolution electron scattering). The design goal of obtaining a transverse phase space limited to $\pi \times 2.5 \times 10^{-3}$ cm-mrad was assumed to be adequate. This value would be approximately 10 times the transverse phase space defined by the apertures in the 80 keV system.

Calculations^{4,6} showed that if the 80 keV electrons injected into the capture section did fall within our design limit of $\pi \times 10$ mm-mrad ($\pi \times 5 \times 10^{-4}$ cm-mrad) the increase in the effective longitudinal phase space would be insignificant, and that the growth in the effective transverse phase space would be a factor of about 1.4. The transverse growth from the transport through the beam filter³ was calculated to be a factor of 2.4.

Measurements

Both the transverse and longitudinal phase spaces from the 80 keV system were measured and were found to be well within our design limits. The phase spread was measured by employing another TM₁₂₀ cavity to produce a phase dependent deflection which was measured with a wire profilometer and also observed on a phosphor screen. For currents to 100 μ a, 90% of the beam was contained in the longitudinal and transverse phase space areas $\pi \times 3.5$ keV-deg and $\pi \times 5$ mm-mrad ($\pi \times 2.5 \times 10^{-4}$ cm-mrad) respectively.

The field gradients attainable in the accelerator so far are limited to about 3 MV/m. In order to have effective capturing and bunching this requires either shortening the capture section to lower its wave velocity, or increasing the incident energy of the electrons. Both will ultimately be done but for these measurements the gun was operated at 90 kV and the prebuncher cavity was operated so that, in addition to bunching the beam, an energy gain of 17 keV was realized. Figure 3 shows the measured effect of the incident energy and field gradient on the output energy. A low output energy will also be accompanied by poor bunching and, what is worse, an unmanageable phase-space shape. The curves of Fig. 3 agree with calculated values except for a few percent in absolute calibration.

With the phasings of the cavities and accelerator structures adjusted for a minimum in the spread in energy, a spread of 3.6 keV (FWHM) was achieved ($E/E = 0.045\%$). Shown in Fig. 4 is the energy spectrum of the 8 MeV beam. Also shown is the phase spectrum from the injector which has been converted to an energy spectrum by a 6 meter superconducting accelerating section operating as a phase analyzer. With the dispersion of the phase analyzer-set at 10 keV/degree, the width of the spectrum (FWHM) was 30 keV, which corresponded therefore to a phase spread of 3 degrees (FWHM). These measurements were made at a current of 10 μ a (CW). We were able to accelerate currents up to 290 μ a (CW) but were not able to make high resolution measurements above 15 μ a because of the onset of beam breakup instabilities⁷ in the superconducting phase analyzer.

The transverse phase space of the electron beam at 8 MeV was determined by measuring the diameter of the beam spot at a focus and at a measured distance from the focus. At least 90% of the 8 MeV electrons were contained in the transverse phase space of $\pi \times 0.3$ mm-mrad. This value represented an expansion by a factor of two in the effective transverse phase-space area injected into the capture section. These measurements were made with the beam by-passing the beam filter which was not fully operational. The beam filter is

expected to be fully operational for our next testing of the system.

It should be noted that the excellent stability of the beam energy (better than 10^{-4} short term) and the 0.045% FWHM energy spectrum demonstrated well the performance of the rf control system which stabilizes the amplitudes and phases of the rf fields in the superconducting structures. A one degree shift in the rf phase of the preaccelerator relative to the capture section, for example, will shift the output energy 0.2%. The fluctuations in this rf phase were, therefore, less than 0.2 degree.

Analysis of Results and Computer Simulations

After the last series of tests on the injector system (the beam filter was not yet fully operational), further calculations on the capturing and accelerating process were performed. One objective was to analyze in more detail the operating mode in which the prebunching cavity was used both to provide energy gain and to bunch. Another objective was to determine what improvements in the capture properties could be realized for accelerating gradients in the 2.6 to 3.0 MV/m range if a lower wave-velocity capture section were utilized.

In Fig. 5 are shown the calculated output energies and phases for our present capture section (wave velocity $\beta_w = .995$) for the conditions of 3.3 MV/m and 107 keV electrons injected with an energy and phase spread of ± 1 keV and ± 5 deg, respectively. The basic shape of the phase-space distribution is quite similar to the shape obtained in the calculation for 10 MV/m (3 MV/ft) which was shown in Fig. 2. Typically as the gradient is lowered, the "major" axis of the phase-space distribution is lengthened and the "minor" axis is contracted (effective phase-space area remaining virtually constant).

In order to examine a range of operating conditions for the injector system a computer simulation was performed in which an electron initialized at the input to the prebuncher cavity, was "taken through" the prebuncher, capture section, and preaccelerator section. The variables were the energy of injection into the capture section (gun voltage plus any gain from the prebunching cavity), field gradient for the capture section, prebuncher voltage (peak), and the relative phases between the cavities. The preaccelerator was assumed to operate at the fixed gradient of 2.5 MV/m. In Table I the spreads in energy and phase are listed for various choices of the parameters. The initial input phase space (longitudinal) was limited to ± 150 volts and ± 20 degrees (25 electrons with energies 0, ± 75 , and ± 150 volts and phases 0, ± 10 , ± 20 deg). The maximum spreads and the rms deviations (equal weighting for each electron) of the phase and energy were computed. The remaining variables were adjusted to minimize the total spread in energy (the preaccelerator was therefore phased so that phase-space distribution from the capture section was "sheared" along the energy axis to give a "righted" distribution). The effective phase-space area is approximated by the product $\Delta\theta \times \Delta E$. The input phase-space area is 12 keV-degrees. For all the cases except the first one in Table I, the prebuncher was at -90 degrees with respect to the (0,0) electron (no energy gain to this electron). For case #1 the prebuncher is phased at -8 degrees (the 0,0 electron gets almost a 17 keV boost). This case is basically the mode of operation that was used in the last injector test. Also in Table I are presented the results of a proposed capture section with wave velocity $\beta_w = 0.95$.

TABLE I

#	β_w	K.E. (in) keV	Gradient Capt. MV/ft.	K.E. (Out) Capt. MeV	$\Delta\theta$ Deg	$\Delta\theta$ (rms) Deg	ΔE keV	ΔE (rms) keV	$\Delta E \cdot \Delta\theta$ keV-Deg.
1 *		107	1.0	2.0	5.1	3.1	16.8	8.2	86
2		107	1.0	2.0	3.8	2.1	6.1	3.2	23
3		100	1.0	1.8	3.6	2.2	6.1	3.0	22
4	.995	90	1.0	1.5	4.5	2.4	6.4	3.1	29
5		90	0.9	1.1	7.0	3.6	12.2	6.3	85
6		120	0.8	1.4	4.0	2.5	6.1	3.2	24
7		100	0.8	0.9	6.2	3.5	12.6	5.4	78
8		100	1.0	2.5	3.1	1.6	4.7	2.5	15
9		90	0.9	2.1	3.1	1.8	5.7	3.2	18
10		80	0.9	1.9	2.9	1.6	6.1	3.5	18
11	.950	100	0.8	1.8	3.2	1.7	4.9	2.4	16
12		90	0.8	1.7	3.1	2.0	5.6	2.8	17
13		80	0.8	1.4	5.1	2.5	9.3	5.5	47

* Prebuncher phase at -8 degrees from peak voltage gain (gun @ 90 kV)

It is evident from Table I that when the pre-buncher cavity is used to boost the input energy (case #1), the effective area of the longitudinal phase space is increased significantly. At 8 degrees off of the peak, simple bunching no longer occurs when the input spread is ± 20 degrees. For the same input energy and capture section field gradient as in case #1, a large improvement occurs if the gun voltage is increased to 107 keV and pre-buncher voltage is reduced to produce "good" bunches (case #2). If the input energy of the field gradient of the capture section gets too low (as in case #5) the phase space deteriorates quickly. For the field gradients and gun voltages considered, for a $\beta_w = .95$ capture section not only are effective phase-space areas smaller but also there are substantial increases in the energy gain.

In our next testing of the injector system we plan to increase our gun voltage to 105 kV so that we may operate at field gradients in the capture section of 3.0 MV/m (0.9 MV/ft) and still obtain an excellent longitudinal phase space at the output. The beam filter will be tested and the isochronism verified. By controlling the focal length of solenoidal lens located between the second and third bending magnets (see Fig. 1), we should be able to adjust the phase versus energy correlation over a range of ± 20 degrees per $\% \Delta E/E$. This enables us to "shear" a phase space distribution in the phase direction. The phase-space distribution in Fig. 4, for example, could be sheared along the energy axis by the preaccelerator and then sheared along the phase axis to produce a "righted" distribution one degree wide and 20 keV high.

We will be able to examine phase spaces at currents up to 200 μ a. At the 200 μ a level we expect to see a little growth in the transverse phase space from space charge forces. We estimate however that space charge forces should not significantly increase the longitudinal phase space at the 200 μ a level.

Conclusion

The testing and analysis of the injector for the Stanford superconducting linac indicates that a longitudinal space distribution with a phase spread of 1 degree FWHM and an energy spread 10 keV FWHM can be achieved. This would mean that a $\Delta E/E < 2 \times 10^{-4}$ FWHM could be achieved at 100 MeV for the linac. With the present capture section it would be necessary to increase the gun voltage to more than 120 kV in order to guarantee this performance for field gradients as low as 2.6 MV/m (0.8 MV/ft). For a $\beta_w = 0.95$ capture section operating at this field gradient, a 90 kV gun voltage would be adequate. Our present gun system is capable of operating to approximately 100 kV.

In the next test of the injector system we will verify the performance of the beam filter. We will also extend our phase-space measurements to beam currents greater than 100 μ a.

References

- * Work supported in part by the National Science Foundation and the Office of Naval Research.
- 1 H. A. Schwettman, J. P. Turneaure, W. M. Fairbank, T. I. Smith, M. S. McAshan, P. B. Wilson, and E. E. Chambers, IEEE Trans. Nuc. Sci., NS-14, 336 (1971).
- 2 L. R. Suelzle, Status of the Superconducting 2 GeV Linear Electron Accelerator, IEEE Trans. Nuc. Sci., NS-18, 146 (1971).
- 3 E. E. Chambers, Conclusions of Computer Study of Superconducting Capture and Preaccelerator Sections and Design of Beam Filter and Collimator System, Stanford High Energy Physics Laboratory Technical Note HEPL TN-70-2 (1970).
- 4 E. E. Chambers, Electron Optics of the Capture Section of the Superconducting Accelerator, Stanford High Energy Physics Laboratory Technical Note HEPL TN-71-2 (1971).
- 5 J. Haimson, Optimization Criteria for Standing Wave Transverse Magnetic Deflection Cavities, Proceedings of the 1966 Linear Accelerator Conference, Los Alamos (LA 3609), p. 303.
- 6 E. E. Chambers, Particle Motion in a Standing-wave Linear Accelerator, Proc. 1968 Summer Study On Superconducting Devices and Accelerators, Part I, BNL 50155 (C-55) Brookhaven National Laboratory, 1968) p. 67.
- 7 K. Mittag, H. A. Schwettman, and H. D. Schwarz, Beam Breakup in a Superconducting Linear Electron Accelerator (to be published in the Proceedings of the 1972 Linear Accelerator Conference, Los Alamos).

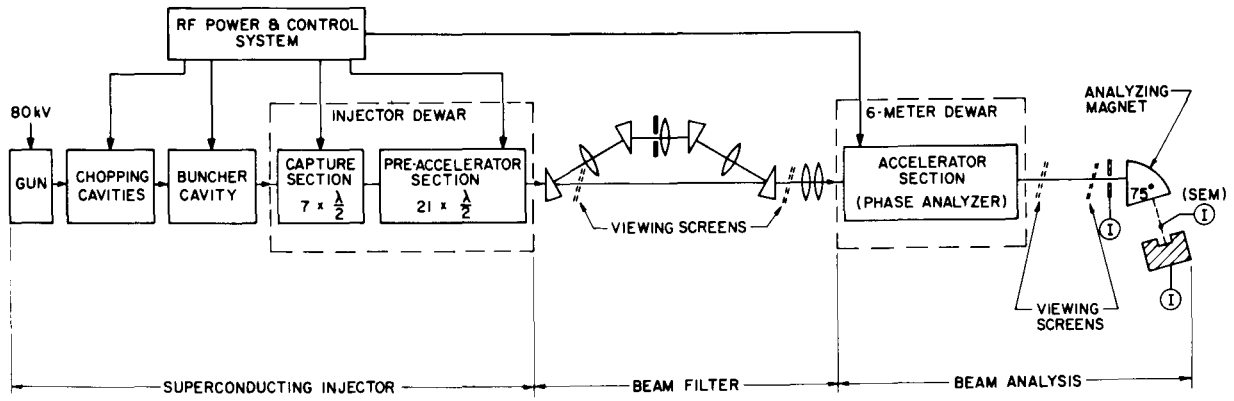


Fig. 1. Schematic diagram of superconducting injector and beam analysis system.

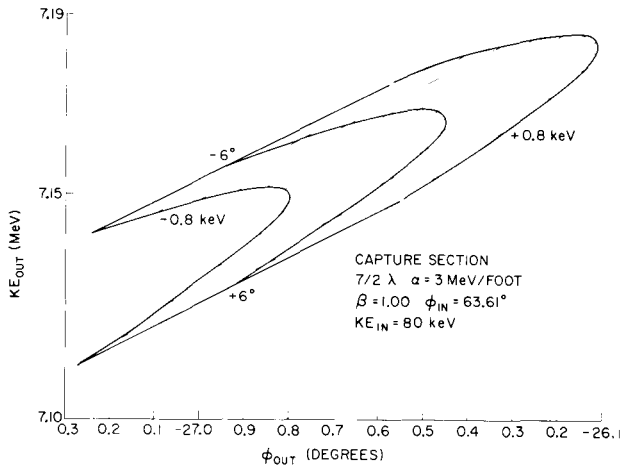


Fig. 2. Calculated capture properties for a $\beta_w = 1.0$ capture section at 10 MV/m and 80 keV injection.

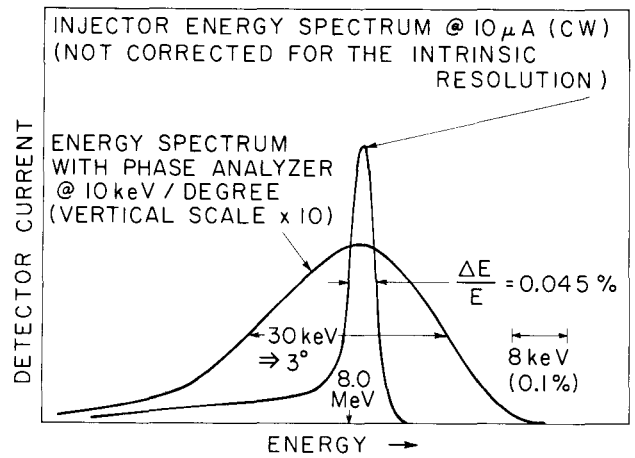


Fig. 4. Energy spectra obtained from the injector at 8 MeV.

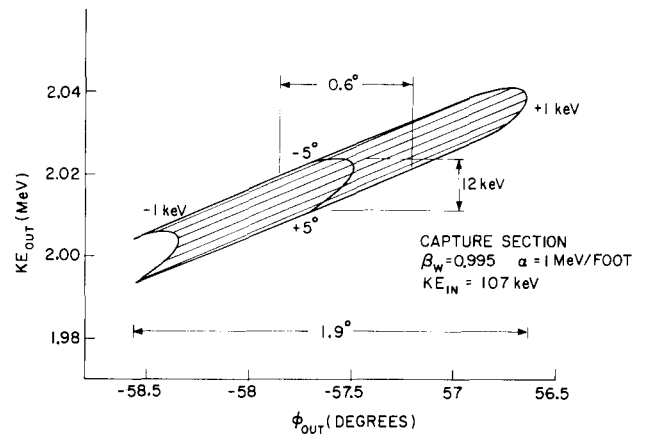
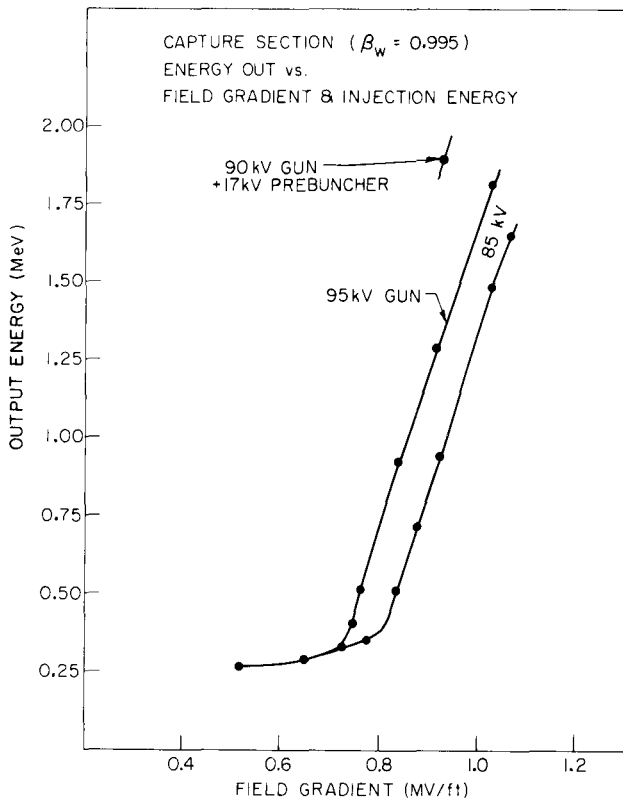


Fig. 5. Calculated capture properties for a $\beta_w = 0.995$ capture section at 3.3 MV/m and 107 keV injection.

Fig. 3. Measured output energy from a $\beta_w = 0.995$ capture section versus the injection energy and field gradient.